

An Automated Approach for Change Detection in Mars Time-Series Images from Online Image Archives using Web Crawler and Deep Learning

Shuo Liu, Bo Wu*, Ran Duan, Sergey Krasilnikov

Research Centre for Deep Space Explorations | Department of Land Surveying & Geo-Informatics, The Hong Kong Polytechnic University, Hung Hom, Kowloon, Hong Kong – bo.wu@polyu.edu.hk

Keywords: Mars, time-series images, change detection, web crawler, deep learning

Abstract

Mars is a dynamic planet exhibiting numerous active surface phenomena, such as recurring slope lineae (RSL), commonly seen on the Martian surface in the mid-latitude regions. Automatic detection of these changes on the Martian surface is pivotal for understanding the evolution and dynamic processes of Mars. Deep-learning models for change detection, such as the Siamese network, have been widely used for identifying changes in images. This paper presents a deep-learning model based on the backbone of the Siamese network, incorporating a spatial attention module and a balanced evaluation method, for detecting dynamic changes on the Martian surface from time-series images. Moreover, we developed a multi-processing web crawler for automatic data retrieval and processing from online image archives, significantly enhancing the efficiency and reach of the change detection method. The effectiveness and reliability of the proposed method have been validated using real time-series Mars images covering typical regions on the Martian surface, focusing on the detection of a typical dynamic phenomenon on Mars, i.e., RSL. The proposed method can automatically retrieve and process data from online image archives, such as the High Resolution Imaging Science Experiment (HiRISE) image archives, and achieves a change detection accuracy of 81.8%. Results indicate that the method can detect subtle changes on the Martian surface from online image archives automatically, showing promising potential for studying the dynamic environment of Mars and enhancing our understanding of Martian surface dynamics.

1. Introduction

Mars is a planet characterized by a variety of dynamic activities. Detecting changes on its surface is essential for comprehending the planet's dynamic processes, geological history, and climate evolution. For example, tracking changes like new impact craters helps scientists refine models of the Mars surface age and history (Daubar et al., 2013). Furthermore, identifying changes aids in the search for water, a crucial component for life, by pinpointing areas of interest such as recurring slope lineae (RSL), which might suggest temporary liquid water flows (Ojha et al., 2015). Thus, detecting changes on Mars offers a dynamic perspective of the planet, uncovering processes that static observations cannot reveal.

Detecting surface features and changes on planetary surfaces typically relies on various types of remote sensing data, such as images and digital elevation models (Wu et al., 2021a; Ye et al., 2021). Image data from Mars orbiter cameras, including the High Resolution Imaging Science Experiment (HiRISE) (McEwen et al., 2007), the Context Camera (CTX) (Bell et al., 2013; Malin et al., 2007), and the Compact Reconnaissance Imaging Spectrometer for Mars (CRISM) (Murchie et al., 2007) aboard the Mars Reconnaissance Orbiter (MRO), are essential for change detection on the Martian surface. HiRISE images (0.3 m/pixel) are better suited for examining small-scale surface changes. CTX images (6 m/pixel) cover large areas, making them suitable for large-scale change detection, while CRISM is crucial for spectral analysis and mineral detection in research areas.

Web crawlers are effective tools for searching and downloading images from websites, overcoming the challenges of navigating vast amounts of web content by quickly extracting and indexing information on a large scale, which manual downloading cannot achieve (Olston & Najork, 2010). Therefore, developing a web crawler for long-term and large-scale detection is crucial for managing large data volumes.

Additionally, automatically detecting features such as RSL and their changes on Mars is challenging due to their subtle nature, with widths ranging from 0.5–5 m (McEwen et al., 2011). Traditionally, RSL were manually labeled (e.g., Stillman, 2018; Mitchell & Christensen, 2016), which is a time-consuming and labor-intensive task. To address this, Stillman et al. (2020) developed the Mapping and Automated Analysis of RSL (MAARSL) method to facilitate automatic RSL detection. However, despite its efficiency compared to manual labeling, MAARSL still requires human intervention to ensure accurate and reliable results. This underscores the need for improved methods that can automatically, efficiently, and accurately identify dynamic changes from online data archives with minimal manual input.

In this paper, we introduce an innovative method for automatically detecting changes from time-series images of Mars. Our approach uses a web crawler to automatically retrieve time-series data from online archives such as HiRISE, CTX, and CRISM, based on the location of the specific research area. Once the necessary data are downloaded, change detection is performed using a deep-learning method based on an enhanced Siamese network. We validated this approach by automatically retrieving HiRISE data and detecting RSL in the mid-latitude regions on Mars. Additionally, we evaluated the efficiency of the automatic data retrieval process and the accuracy of the Siamese network model.

The rest of this paper is structured as follows: Section 2 describes the method for automatic change detection from time-series images of Mars. Section 3 details the experimental evaluation using RSL as a case study. Finally, Section 4 offers concluding remarks and further discussion.

2. Automatic Workflow for Change Detection in Mars Time-Series Images

2.1 Framework of the Approach

Figure 1 presents the workflow of the approach. Starting with data retrieved by the Web crawler, which searches relevant websites based on specific requirements to gather data. Simultaneously, a target time range is established using Mars Year as its unit, which is crucial for detecting temporal changes, and metadata along with georeferenced information are collected to register and compile time-series data. The compiled data are then input into the Siamese network, which consists of two channels, each dedicated to processing images from different time periods. By sharing weights between the two channels, the network can effectively compare feature maps. To improve feature extraction, each channel is followed by an attention module. The processed outputs are then passed to an up-sampling component that employs a U-Net architecture for pixel-by-pixel reconstruction, with the results normalized for further analysis. Finally, the system assesses the accuracy of the proposed model and generates a binary mask to highlight areas of interest or change. The output is a binarized mask that outlines changed areas on the Martian surface, aligning well with the high-resolution satellite images processed by the Siamese network.

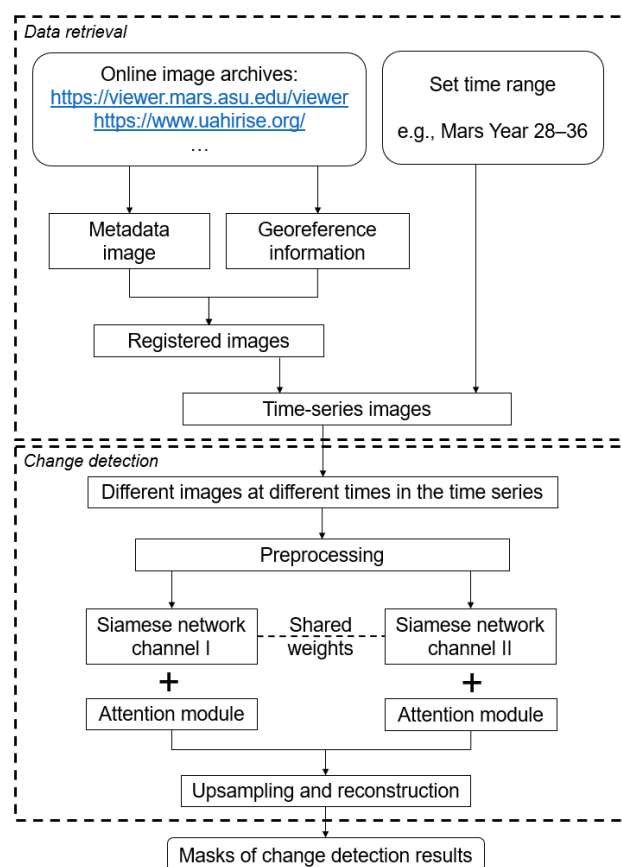


Figure 1. Workflow of the proposed approach.

2.2 Web crawler for Automatic Data Retrieval from Online Image Archives

The process of retrieving and downloading data with a Web crawler encompasses a series of crucial steps aimed at methodically and effectively gathering information from the Internet (as illustrated in Figure 2). To begin with, based on the information about the target area and the specific dataset required,

the crawler generates target product names based on the location and established naming conventions for each product. Following this, the crawler compiles a list of precise URLs, which are then fed into the crawler frontier to guide the data collection process. To mitigate any potential disruptions during downloading, a retry mechanism is incorporated, ensuring the program operates smoothly without interruptions. Once the data is successfully downloaded, image matching is conducted using tie points (Hu et al., 2016; Li et al., 2008). Subsequently, image registration is performed to either link different images together or to georeference the images to a base map (Wu et al., 2013; 2015). The outcomes are usually stored in a structured format for subsequent analysis and are then securely stored in a designated data repository. This comprehensive approach not only ensures the accuracy and reliability of the collected data but also facilitates easy access and management for future use.

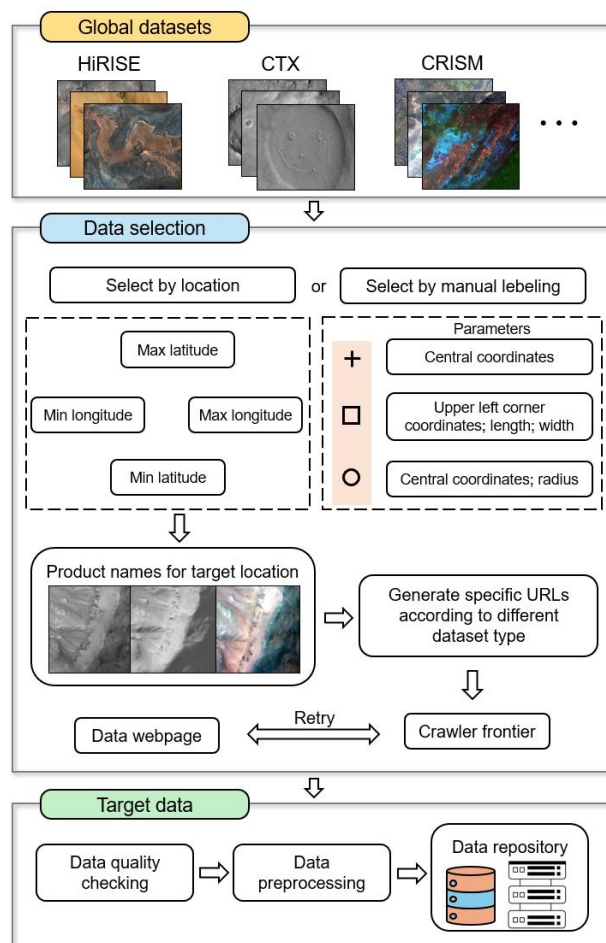


Figure 2. Workflow for automatic online data retrieval, preprocessing, and storage.

In the realm of Web crawling, implementing retry mechanisms is essential for ensuring robust and dependable data collection. Web crawlers often face temporary challenges like network timeouts, server errors, or webpages being momentarily unavailable (Olston & Najork, 2010). A well-designed retry strategy enables crawlers to effectively manage these issues, thereby enhancing the overall success rate of data retrieval (Pant et al., 2004). The retry mechanism involves making multiple attempts to access a web resource after an initial failure, typically with a pause between tries (Grimes et al., 2008). This method can greatly improve a crawler's resilience by allowing it to navigate temporary disruptions. For example, exponential backoff, a

widely used retry strategy, increases the wait time between consecutive attempts, reducing server load and minimizing the likelihood of repeated failures (Al Galib et al., 2024). Additionally, incorporating retry logic helps ensure compliance with website terms of service by avoiding excessive requests in a short timeframe (Pardon & Pautasso, 2014). By effectively managing retries, Web crawlers can achieve more reliable and efficient data collection, ultimately resulting in more accurate and comprehensive datasets.

The proposed method for the data downloading using Web crawler follows the detailed and specific sequence of steps: Initially, by pinpointing the exact location of the target area, the orbit number and target code can be swiftly determined. The target code indicates the latitudinal position of the center of the intended observation area in relation to the beginning of the orbit. For instance, in the case of HiRISE, the first six digits of the target code correspond to the orbit number, with the orbit commencing at the equator on the descending (night) side. The subsequent three digits represent the number of complete degrees from the orbit's start, while the fourth digit indicates the fractional degree, rounded to the nearest half-degree. Data from sources like HiRISE can be easily located and downloaded using the generated product name and URL. Conversely, for data from other sources such as CTX, the inferred product names cannot be directly utilized to create the target URLs. Additionally, some Asynchronous JavaScript XML (AJAX) requests require crawling a completely new URL and volume ID for data retrieval, which demands more preparation time and may slow down the downloading process.

2.3 Spatial Attention-Enhanced Siamese Network for Change Detection

Traditional machine learning approaches for object detection, like the use of support vector machines combined with the

histogram of oriented gradients employed by Wang et al. (2021) to identify surface features on Mars, are effective when working with limited training samples and simpler machine learning networks (Wu et al., 2021b). However, the Siamese network is a deep learning architecture specifically crafted for change detection by assessing the similarity between two images. Typically, it produces one-dimensional outputs, such as a similarity score that quantifies the resemblance between the input images (Bromley et al., 1993). In this paper, U-Net is chosen as one of the backbone networks for the proposed framework, especially for the upsampling and reconstruction part. It then reconstructs the results on a pixel-by-pixel level through up-sampling, facilitating accurate change detection at the pixel level. This capability makes U-Net particularly suitable for tasks requiring detailed analysis of image differences, as it ensures that even subtle changes are captured and represented accurately. By leveraging the strengths of both the Siamese network and U-Net, the framework is well-equipped to handle complex change detection tasks, providing robust and precise results that can be applied in various fields such as remote sensing, medical imaging, and environmental monitoring.

Figure 3 illustrates the network architecture utilized in this paper. This framework takes as input two images that display certain variations taken in different time periods. After adjusting the size to match the performance capabilities of different computers, these images are separately processed through a U-Net architecture, where they undergo down-sampling to progressively extract pertinent information with sharing weights with each other, which are applied to the images. Following this, the distinct features of the two images are up-sampled to generate change detection results, which are then compared against the input label. The loss function is employed to measure the discrepancy between the two images and the input label, and the weights and bias are adjusted accordingly to improve accuracy.

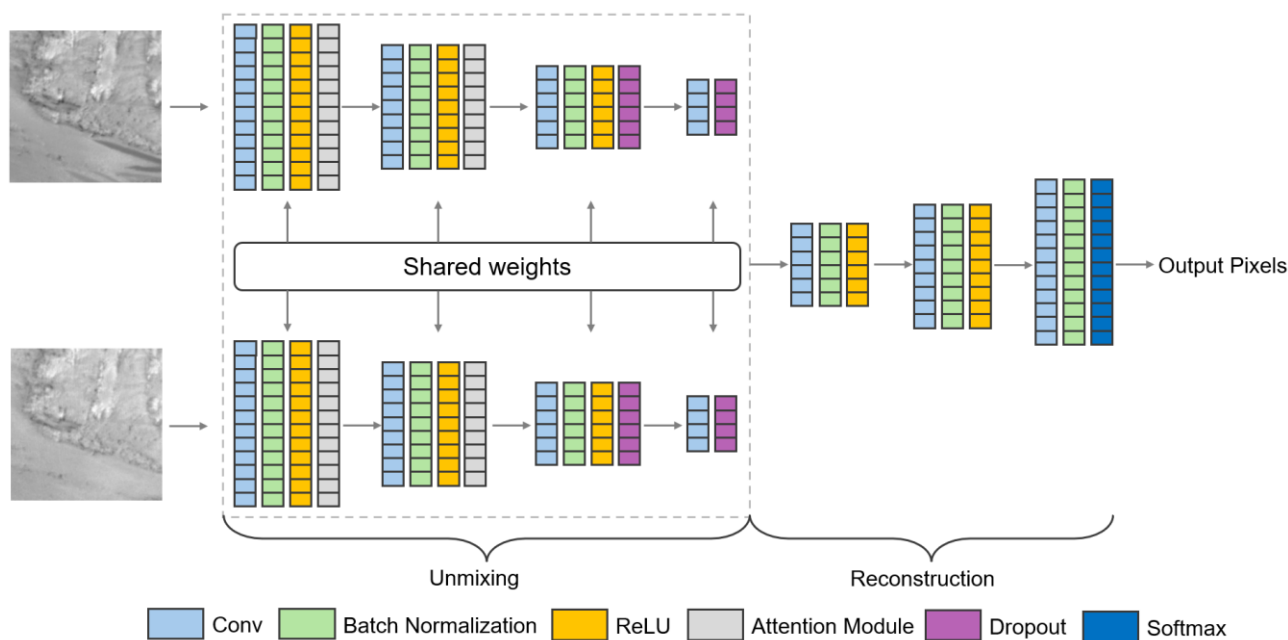


Figure 3. Structure of Siamese network, with the inputs being images at different time points and the output being pixel-by-pixel change detection results.

Considering the variations in surface features and the imbalanced nature of the image background, a spatial attention module is implemented to address the imbalance between positive and

negative samples. This module is a specialized module designed to modulate the response feature values across the spatial dimension (Zhang et al., 2022). It amplifies relevant information

while reducing the influence of extraneous data, thereby addressing the typical lack of contextual information found in traditional convolutional approaches. By enabling a single feature at any position to perceive features from all other positions, this module enhances the robustness of pixel-by-pixel representation capabilities. The spatial attention module is often visualized as a probability map or feature vector, assigning higher weights to spatial positions that necessitate the extraction of positive information. Depending on the specific task at hand, the regions emphasized by the spatial attention module within the same image may differ, allowing for a more tailored and effective analysis. This approach not only improves the detection of meaningful changes but also enhances the overall performance of the network in various image processing tasks.

3. Experimental Analysis

As a common dynamic feature on the Martian surface, RSL was chosen as a case study to test the effectiveness of the developed method. RSL are typically narrow, with widths ranging from 0.5 to 5 meters and lengths possibly exceeding 100 meters (McEwen et al., 2011). Detection of RSL requires high-resolution orbital images, such as those provided by HiRISE. As a sun-synchronous orbiter (Zurek & Smrekar, 2007; Thomas et al., 2010), HiRISE is capable of capturing multi-temporal surface images with nearly identical solar incidence and emission angles, minimizing significant differences in features like hill shading between images. RSL can be distinguished from their surroundings by several morphological and spectral characteristics: (i) narrow, elongated shape (Bhardwaj et al., 2019); (ii) originate at bedrock outcrops (McEwen et al., 2011) and flow down steep slopes (Munaretto et al., 2020); (iii) lower albedo (McEwen et al., 2014; Ojha et al., 2014) or spectral reflectance (Ojha et al., 2015) than that of the surrounding terrain; (iv) longest during the summer and gradually vanish afterward, showing a recurring annual cycle (Vincendon et al., 2019).

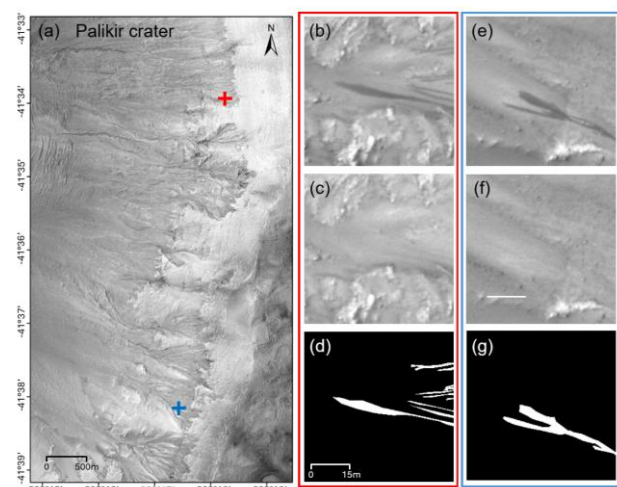


Figure 4. (a) Part of Palikir Crater ($-41^{\circ}35'$, $202^{\circ}10'$). (b, c, d) (e, f, g) are two groups of training sample showing appearance and disappearance of RSL across different seasons. (d, g) Input label for training and accuracy verification.

The proposed method allows for efficient detection of RSL. Initially, HiRISE images from various time periods are automatically retrieved from the online image archive based on the longitude and latitude of the target areas. Next, the proposed deep-learning model, using training samples (Figure 4), generates a feature map for detecting changes on a pixel-by-pixel basis. Finally, by converting the feature map into a binary format,

the changed areas are marked as white regions, which are well aligned with those in high-resolution images taken at the same or similar solar longitude. This approach streamlines the process of identifying RSL, ensuring accurate mapping and analysis of these dynamic Martian features.

The HiRISE data from Palikir Crater during the summer and autumn of Mars Year 31 were divided into 256×256 square patches, with 70% used for training and 30% reserved for validation. A pixel-based evaluation method was employed to qualitatively assess the model's performance (Figure 5). Although there are some inaccuracies in detecting the edges of RSL, the model significantly reduces the effort required for manually labeling RSL.

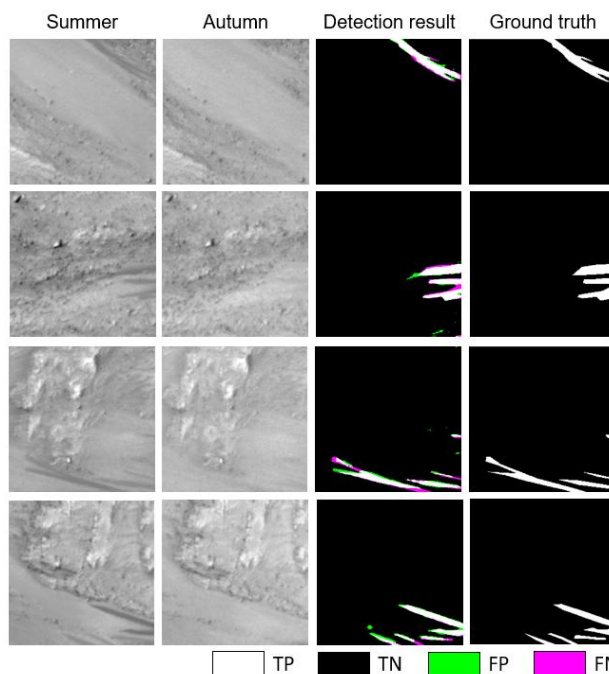


Figure 5. Visualization of evaluation results. Columns 1 and 2: Summer and autumn HiRISE images; Column 3: Detection results; Column 4: Ground truth for evaluation and comparison. TP, TN, FP, FN means true positive, true negative, false positive and false negative separately.

Due to slight variations in solar incidence angles and georeferencing issues with HiRISE images, small hill shades may occasionally be misidentified as RSL during detection. However, since this error is systematic, it is relatively straightforward to correct. On the other hand, if many RSL are missed, the workload increases exponentially. Therefore, correcting false negatives by adding the missed RSL to achieve accurate results is more challenging than eliminating falsely detected RSL.

Indicator	Results
Sensitivity	64%
Specificity	99.6%
False discovery rate (FDR)	0.4%
Overall accuracy	99%
Balanced accuracy	81.8%

Table 1. Performance metrics of RSL detection model.

Overall accuracy is significantly affected by the large number of negative samples (background), making traditional accuracy evaluation methods unsuitable for situations with a large imbalance between positive and negative samples. In such cases,

a balanced accuracy evaluation method is more reliable. Table 1 provides the quantitative evaluation criteria for the RSL detection model. Given the imbalanced distribution of RSL and background, the balanced accuracy is 81.8%, which is considered sufficient and acceptable for reducing manual workload. False detections mainly occur in small hill shade areas, while the major omissions are at the edges of RSL and in extremely narrow RSL regions, approximately 30 cm (~1 pixel) wide. These narrow RSL have higher I/F (radiance/irradiance) values than wider RSL, making them difficult to distinguish from their surroundings.

4. Conclusions

In this paper, we introduced a novel method that integrates the functionality of a Web crawler with an enhanced Siamese network to identify changes on the Martian surface. To evaluate the effectiveness and precision of this method, we concentrated on the automatic detection of RSL, a subtle and seasonally varying phenomenon on Mars. Using our innovative approach, we performed change detection analyses on RSL across various Martian regions. Our key findings are as follows:

(1) The proposed method successfully retrieves and processes data from online image archives with a 100% success rate, when given a stable network connection and retry mechanism. This automation greatly simplifies the data acquisition process, ensuring researchers have consistent access to high-quality images for analysis.

(2) Our approach's change detection capability achieves a pixel-by-pixel balanced accuracy of 81.8%, significantly reducing repetitive manual tasks. This high level of precision results from thorough training and validation, allowing the model to reliably detect even the most subtle changes on Mars. By reducing the need for human intervention, this method enables more efficient and extensive data analysis.

(3) The method can automatically detect RSL on Mars more efficiently and robustly than manual techniques. This will facilitate a deeper analysis of RSL, including their spatial and temporal patterns, and enhance understanding of the environmental factors affecting their distribution and behavior.

The proposed method highlights the potential to enhance our understanding of Martian surface dynamics by enabling more efficient and comprehensive studies of the planetary changing environment. With automated detection and analysis, researchers can focus on interpreting results and developing new insights into the mechanisms driving changes on Mars. Beyond RSL analysis, this approach shows promise for detecting other dynamic phenomena on Mars, such as ice block movements in polar regions and new impact craters, offering broad applications in planetary research.

Acknowledgements

This work was supported by grants from the Research Grants Council of Hong Kong (Project No: PolyU 15210520, RIF Project No: R5043-19, CRF Project No: C7004-21GF). The authors thank all individuals who worked on the dataset archives to make them publicly available.

References

Al Galib, A., Mehedi, M.H.K., Rhythm, E.R., Rasel, A.A., 2024. Large Scale Web Crawling and Distributed Search Engines:

Techniques, Challenges, Current Trends, and Future Prospects. In Proceedings of the Computing and Informatics, Singapore, 17-29.

Bell, J.F.III, Malin, M.C., Caplinger, M.A., Fahle, J., Wolff, M.J., Cantor, B.A., James, P.B., Ghaemi, T., Posiolova, L.V., Ravine, M.A., Supulver, K.D., Calvin, W.M., Clancy, R.T., Edgett, K.S., Edwards, L.J., Haberle, R.M., Hale, A., Lee, S.W., Rice, M.S., Thomas, P.C., Williams, R.M.E., 2013. Calibration and performance of the Mars reconnaissance orbiter context camera (CTX). *International Journal of Mars Science and Exploration*, 8, 1-14.

Bhardwaj, A., Sam, L., Martín-Torres, F.J., Zorzano M., 2019. Discovery of recurring slope lineae candidates in Mawrth Vallis, Mars. *Scientific Reports*, 9, 2040.

Bromley, J., Guyon, I., LeCun, Y., Säckinger, E., Shah, R., 1993. Signature verification using a "siamese" time delay neural network. *Advances in neural information processing systems*, 6.

Daubar, I.J., McEwen, A.S., Byrne, S., Kennedy, M.R., Ivanov, B., 2013. The current martian cratering rate. *Icarus*, 225(1), 506-516.

Grimes, C., Ford, D., Tassone, E., 2008. Keeping a Search Engine Index Fresh: Risk and optimality in estimating refresh rates for web pages. In Proceedings of the 40th Symposium on the Interface: Computing Science and Statistics, Durham, NC, USA, 1-14.

Hu, H., Ding, Y., Zhu, Q., Wu, B., Xie, L., Chen, M., 2016. Stable least-squares matching for oblique images using bound constrained optimization and a robust loss function. *ISPRS Journal of Photogrammetry and Remote Sensing*, 118, 53-67.

Li, R., Deshpande, S., Niu, X., Zhou, F., Di, K., Wu, B., 2008. Geometric integration of aerial and high-resolution satellite imagery and application in shoreline mapping. *Marine geodesy*, 31(3), 143-159.

Malin, M.C., Bell, J.F., Cantor, B.A., Caplinger, M.A., Calvin, W.M., Clancy, R.T., Edgett, K.S., Edwards, L., Haberle, R.M., James, P.B., Lee, S.W., Ravine, M.A., Thomas, P.C., Wolff, M.J., 2007. Context camera investigation on board the Mars Reconnaissance Orbiter. *Journal of Geophysical Research: Planets*, 112(E5).

McEwen, A.S., Eliason, E.M., Bergstrom, J.W., Bridges, N.T., Hansen, C.J., Delamere, W.A., Grant, J.A., Gulick, V.C., Herkenhoff, K.E., Keszthelyi, L., Kirk, R.L., Mellon, M.T., Squyres, S.W., Thomas, N., Weitz, C.M., 2007. Mars Reconnaissance Orbiter's High Resolution Imaging Science Experiment (HiRISE). *Journal of Geophysical Research: Planets*, 112(E5).

McEwen, A.S., Ojha, L., Dundas, C.M., Mattson, S.S., Byrne, S., Wray, J.J., Cull, S.C., Murchie, S.L., Thomas, N., Gulick, V.C., 2011. Seasonal Flows on Warm Martian Slopes. *Science*, 333(6043), 740-743.

McEwen, A.S., Dundas, C.M., Mattson, S.S., Toigo, A.D., Ojha, L., Wray, J.J., Chojnacki, M., Byrne, S., Murchie, S.L., Thomas, N., 2014. Recurring slope lineae in equatorial regions of Mars. *Nature Geoscience*, 7, 53-58.

- Mitchell, J.L., Christensen, P.R., 2016. Recurring slope lineae and chlorides on the surface of Mars, *Journal of Geophysical Research: Planets*, 121, 1411–1428.
- Munaretto, G., Pajola, M., Cremonese, G., Re, C., Lucchetti, A., Simioni, E., McEwen, A.S., Pommerol, A., Becerra, P., Conway, S.J., Thomas, N., Massironi, M., 2020. Implications for the origin and evolution of Martian Recurring Slope Lineae at Hale crater from CaSSIS observations. *Planetary Space Science*, 187, 104947.
- Murchie, S., Arvidson, R., Bedini, P., et al., 2007. Compact Reconnaissance Imaging Spectrometer for Mars (CRISM) on Mars Reconnaissance Orbiter (MRO), *Journal of Geophysical Research: Planets*, 112, E05S03.
- Ojha, L., McEwen, A.S., Dundas, C., Byrne, S., Mattson, S., Wray, J., Masse, M., Schaefer, E., 2014. HiRISE observations of Recurring Slope Lineae (RSL) during southern summer on Mars. *Icarus*, 231, 365-376.
- Ojha, L., Wilhelm, M.B., Murchie, S.L., McEwen, A.S., Wray, J.J., Hanley, J., Massé, M., Chojnacki, M., 2015. Spectral evidence for hydrated salts in recurring slope lineae on Mars. *Nature Geoscience*, 8(11), 829-832.
- Olston, C., Najork, M., 2010. Web Crawling, Foundations and Trends in Information Retrieval: Vol. 4: No. 3, pp 175-246.
- Pant, G., Srinivasan, P., Menczer, F., Crawling the Web. in Levene, M., Poulouvassilis, A., (Eds.), *Web Dynamics: Adapting to Change in Content, Size, Topology and Use*, Springer, Boston, 2004, 153-178.
- Pardon, G., Pautasso, C., 2014. Atomic distributed transactions: A restful design. In *Proceedings of the 23rd International Conference on World Wide Web*, 943-948.
- Stillman, D. E., 2018. Chapter 2 - Unraveling the Mysteries of Recurring Slope Lineae, in: Soare, R.J., Conway, S.J., Clifford, S.M., (Eds.), *Dynamic Mars*, Elsevier, Cambridge, 2018, 51-85.
- Stillman, D.E., Bue, B.D., Wagstaff, K.L., Primm, K.M., Michaels, T.I., Grimm, R.E., 2020. Evaluation of wet and dry recurring slope lineae (RSL) formation mechanisms based on quantitative mapping of RSL in Garni Crater, Valles Marineris, Mars. *Icarus*, 335, 113420.
- Thomas, N., Hansen, C.J., Portyankina, G., Russell, P.S., 2010. HiRISE observations of gas sublimation-driven activity in Mars' southern polar regions: II. Surficial deposits and their origins. *Icarus*, 205(1), 296-310.
- Vincendon, M., Pilorget, C., Carter, J., Stcherbinine, A., 2019. Observational evidence for a dry dust-wind origin of Mars seasonal dark flows. *Icarus*, 325, 115-127.
- Wang, Y., Wu, B., Xue, H., Li, X., Ma, J. (2021). An improved global catalog of lunar impact craters (≥ 1 km) with 3D morphometric information and updates on global crater analysis, *Journal of Geophysical Research: Planets*, 126 (9), e2020JE006728.
- Wu, B., Guo, J., Hu, H., Li, Z., Chen, Y., 2013. Co-registration of lunar topographic models derived from Chang'E-1, SELENE, and LRO laser altimeter data based on a novel surface matching method. *Earth and Planetary Science Letters*, 364, 68-84.
- Wu, B., Tang, S., Zhu, Q., Tong, K., Hu, H., Li, G., 2015. Geometric integration of high-resolution satellite imagery and airborne LiDAR data for improved geopositioning accuracy in metropolitan areas. *ISPRS Journal of Photogrammetry and Remote Sensing*, 109, 139-151.
- Wu, B., Li, Y., Liu, W.C., Wang, Y., Li, F., Zhao, Y., Zhang, H., 2021. Centimeter-resolution topographic modeling and fine-scale analysis of craters and rocks at the Chang'E-4 landing site, *Earth and Planetary Science Letters*, 553, 116666.
- Wu, B., Dong, J., Wang, Y., Li, Z., Chen, Z., Liu, W.C., Zhu, J., Chen, L., Li, Y., Rao, W., 2021. Characterization of the candidate landing region for Tianwen-1—China's first mission to Mars. *Earth and Space Science*, e2021EA001670.
- Ye, B., Qian, Y., Xiao, L., Michalski, J.R., Li, Y., Wu, B., Qiao, L., 2021. Geomorphologic exploration targets at the Zhurong landing site in the southern Utopia Planitia of Mars, *Earth and Planetary Science Letters*, 576, 117199.
- Zhang, J., Wang, Y., Wang, H., Wu, J., Li, Y., 2022. CNN Cloud Detection Algorithm Based on Channel and Spatial Attention and Probabilistic Upsampling for Remote Sensing Image. *IEEE Transactions on Geoscience and Remote Sensing*, 60, 1-13.
- Zurek, R.W., Smrekar, S.E., 2007. An overview of the Mars Reconnaissance Orbiter (MRO) science mission. *Journal of Geophysical Research: Planets*, 112(E5).